



FLINDERS UNIVERSITY  
College of Science and Engineering

**TRIBOCORROSION BEHAVIOUR OF TITANIUM ALLOYS  
FOR MEDICAL APPLICATIONS**

Submitted in partial fulfilment of the requirements for the Master of  
Engineering Science (Biomedical)

**Author: Helen Ojoma Adejo**

Supervisor: Dr. Reza Oskouei

Date Submitted: 8<sup>th</sup> November 2021

## *Declaration*

I certify that this thesis does not incorporate without acknowledgement any material previously submitted for a degree or diploma in any university; and to the best of my knowledge and belief it does not contain any material previously published or written by another person except where due reference is made in the text.

Signed:

Date: 08/11/2021

## *Acknowledgements*

Firstly, I would like to give my heartfelt thanks to Dr. Reza H. Oskouei for his unstinting support and guidance all through the entire process of this research. His constant motivation, encouragement and admirable work ethic helped me to complete this research to very high academic standards. He was always available and very eager to help where needed and showed a great level of dedication to the research. He was also very eager to share from his vast array of knowledge and expertise and I owe him a debt of gratitude.

Secondly, I would like to extend my sincere gratitude to Mr. Mohsen Feyzi, a PhD student in the team, without whose assistance this research would not have been possible.

Thirdly, my thanks also go to Mr. Tim Hodge for his help during the sample preparation.

I would like to give my most profound thanks to Australia Awards Africa for their faith in me and for the sponsorship of my studies here in Australia, there is no way I would have done this without them.

Finally, I could never thank my friends and family enough for their encouragement, understanding, patience and concern during the challenging but worthwhile period of this research.

## Executive Summary

The demand for materials to replace lost or damaged tissues and organs has been on the increase in recent years because of an ever-increasing aging population and loss of these organs or tissues through trauma or illness. Titanium and its alloys have emerged as leaders in the field of orthopaedic implants because of their good mechanical properties, lower Young's modulus, excellent corrosion resistance and excellent biocompatibility. Another important property that needs to be considered for implants is tribocorrosion (a process of material degradation due to the combined effects of wear and corrosion) and is very common at the hip and knee joints where sliding occurs during the movement of the body. The two most commonly used titanium alloys for biomedical applications are Ti-6Al-4V and Ti-6Al-7Nb and the tribocorrosion properties of Ti-6Al-4V has been studied extensively but not so that of Ti-6Al-7Nb and this is very concerning. This study, therefore, aims to study the tribocorrosion properties of Ti-6Al-4V and Ti-6Al-7Nb. The alloys were received in the as-cast state and electrochemical polarization tests were first conducted on them after appropriate surface preparation in phosphate buffered saline using a Metrohm Autolab potentiostat running on a three-electrode configuration. This was done to investigate the corrosion behaviour of these alloys. Tribocorrosion tests were then performed under anodic conditions using a ball-on-disc tribometer with the alloys as the disc and zirconia as the ball. The tribocorrosion tests were run at four different contact pressures (580.2 MPa, 674.5 MPa, 839.4 MPa and 992.1 MPa) and three different sliding distance (1 mm, 3 mm and 5 mm). During the tests, a constant potential was applied using the Metrohm Autolab potentiostat while also registering the current to measure the effect of the sliding on current. At the end of the tests, characterizations were done using SEM, SEM with EDX, and roughness meter to observe the wear scar and measure the volume loss.

At the end of the tests, it was discovered that Ti-6Al-7Nb had better corrosion resistance properties but poorer tribocorrosion resistance properties on comparing with Ti-6Al-4V. It was also discovered that tribocorrosion resistance reduced with increasing contact pressure and sliding distance for both alloys.



# TABLE OF CONTENTS

## Table of Contents

<b>INTRODUCTION .....</b>	<b>1</b>
<b>Background of the Study.....</b>	<b>1</b>
<b>Aim.....</b>	<b>1</b>
<b>Scope of the Study.....</b>	<b>1</b>
<b>Experimental Methodology.....</b>	<b>1</b>
<b>Structure of the Thesis.....</b>	<b>2</b>
<b>CHAPTER 1 - LITERATURE REVIEW.....</b>	<b>3</b>
<b>1.1 Introduction.....</b>	<b>3</b>
<b>1.2 Biomaterials.....</b>	<b>3</b>
1.2.1 Metallic Biomaterials used for Load-Bearing Implant Applications .....	3
<b>1.3 Titanium and its Alloys.....</b>	<b>4</b>
1.3.1 Mechanical Properties of Titanium and its Alloys.....	5
1.3.2 Biocompatibility of Titanium and its Alloys.....	6
1.3.3 Corrosion of Titanium and its Alloys.....	7
1.3.4 Wear Behaviour of Titanium and its Alloys.....	8
1.3.5 Tribocorrosion of Titanium and its alloys.....	8
<b>1.4 Research Gap.....</b>	<b>9</b>
<b>CHAPTER 2 - METHODOLOGY.....</b>	<b>11</b>
<b>2.1 Introduction.....</b>	<b>11</b>
<b>2.2 Sample Preparation.....</b>	<b>11</b>
<b>2.3 Electrochemical Corrosion Tests.....</b>	<b>12</b>
2.3.1 Open Circuit Potential (OCP) Measurements.....	13
2.3.2 Potentiodynamic Polarization Tests.....	13
<b>2.4 Tribocorrosion Tests.....</b>	<b>14</b>
2.4.1 Tribocorrosion Tests under Potentiostatic Conditions.....	15
<b>2.5 Surface Characterization.....</b>	<b>15</b>
2.5.1 SEM with EDX Analyser.....	15
2.5.3 Surface Roughness Measurement.....	17
<b>CHAPTER 3 - RESULTS.....</b>	<b>18</b>
<b>3.1 Introduction.....</b>	<b>18</b>
<b>3.2 Electrochemical Corrosion Results.....</b>	<b>18</b>
<b>3.2 Tribocorrosion Results.....</b>	<b>19</b>
3.2.1 Tribocorrosion Graphs.....	19
3.2.2 Mean Current due to Tribocorrosion.....	23
<b>3.3 Surface Roughness.....</b>	<b>25</b>

3.4 SEM Imaging Results .....	28
3.5 EDS Results .....	30
<b>CHAPTER 4 - DISCUSSION.....</b>	<b>32</b>
4.1 Introduction .....	32
4.2 Corrosion Behaviour Analysis .....	32
4.3 Tribocorrosion Behaviour Analysis .....	32
4.4 Surface Characterization .....	33
4.5 Limitations .....	33
5.1 Conclusions .....	34
5.2 Recommendations for Future Work.....	34
<b>REFERENCES .....</b>	<b>35</b>

## Table of Figures

Figure 1: Components of total hip replacement [10] .....	4
Figure 2: Basic concept of tribocorrosion [36] .....	9
Figure 3: Buehler Isomet saw .....	11
Figure 4: Prepared sample .....	12
Figure 5: Electrochemical chamber for polarization tests .....	12
Figure 6: Tribocorrosion test setup .....	14
Figure 7: SEM instrument.....	16
Figure 8: Roughness meter .....	17
Figure 9: Polarization curve for Ti-6Al-4v and Ti-6Al-7Nb in PBS.....	18
Figure 10: Current evolution with time of studied alloys at 5 mm sliding distance and all contact pressures.....	20
Figure 11: Current evolution with time of all alloys at 3 mm sliding distance and all contact pressures.....	21
Figure 12: Current evolution with time of studied alloys at 1mm sliding distance and all contact pressures.....	22
Figure 13: Graphical representation of mean current due to sliding .....	24
Figure 14: Chemical wear volume loss.....	25
Figure 15: Cross-section of wear tracks.....	26
Figure 16: Mechanical Wear volume loss of studied alloys .....	27
Figure 17: SEM images of unworn alloy surfaces with Ti-6Al-4V on the left and Ti-6Al-7Nb on the right .....	28
Figure 18: SEM images for worn surface at 992.1 MPa and 5 mm sliding distance with Ti-6Al-4V on the left and Ti-6Al-7Nb on the right .....	29
Figure 19: SEM images for worn surfaces at 580.2 MPa and 5 mm sliding distance with Ti-6Al-4V on the left and Ti-6Al-7Nb on the right .....	29
Figure 20: SEM images of worn surface at 992.1 MPa and 1 mm sliding distance with Ti-6Al-4V on the left and Ti-6Al-7Nb on the right .....	29
Figure 21: EDS analysis for unworn surface of studied alloys with Ti-6Al-4V on the left and Ti-6Al-7Nb on the right.....	30

Figure 22: EDS analysis for worn surface of studied alloys with Ti-6Al-4V on the left and Ti-6Al-7Nb on the right..... 30

## Table of Tables

Table 1: Mechanical properties of human bone [21] .....	5
Table 2: Mechanical properties of some metallic biomaterials [9].....	6
Table 3: Operating parameters for SEM-EDX .....	16
Table 4: Mean Current due to sliding .....	23
Table 5: Chemical Wear Loss Values.....	24
Table 6: Mechanical wear loss values .....	26
Table 7: Total Wear Loss Values.....	27
Table 8: Total wear loss graph.....	28
Table 9: Chemical composition of unworn Ti-6Al-7Nb.....	30
Table 10: Chemical composition of worn Ti-6Al-7Nb.....	30
Table 11: Chemical composition of worn and unworn Ti-6Al-4V .....	31

## Table of Equations

Equation 1: Passivation equation for Ti.....	7
Equation 2: Chemical wear loss equation.....	24
Equation 3: Wear volume equation.....	25
Equation 4: Equation for R .....	25
Equation 5: Total volume equation.....	27



## INTRODUCTION

**Background of the Study** – Titanium and its alloys have been used in many load-bearing orthopaedic applications because of their exceptional blend of unique properties: good mechanical properties, excellent biocompatibility and impressive corrosion resistance [1, 2]. Ti-6Al-4V has been the most widely used alloy because of its excellent corrosion resistance properties [3], however, because of the presence of aluminium and vanadium, it has been found to be toxic to living cells [4, 5]. Consequently, Ti-6Al-7Nb has been considered as an alternative [3] and has been used quite extensively, however, all its properties have not been fully investigated. Amongst these properties is its tribocorrosion resistance which is concerning, especially in load-bearing applications [6] because the combined effect of wear and corrosion can lead to the release of wear debris which can cause allergic reactions, tissue inflammation and reduction in lifespan of implants [7]. The lack of information on the tribocorrosion behaviour of this alloy means that there is no clear understanding of its behaviour in the presence of the combined effects of wear and corrosion.

**Aim** - The aim of this research was to study the tribocorrosion behaviour of Ti-6Al-7Nb in a bid to provide further insight into the behaviour of this alloy especially in load-bearing applications and evaluate how it compared to the conventional Ti-6Al-4V whose tribocorrosion behaviour has been extensively studied.

**Scope of the Study** – The focus of this study was to investigate the corrosion and tribocorrosion behaviour of Ti-6Al-7Nb alloy and the conventional Ti-6Al-4V. To do this, tests were carried out on both alloys under the same conditions to simulate those encountered by these alloys when implanted into the human body. The major conditions of interest were corrosion and wear conditions.

**Experimental Methodology** – The titanium alloys (Ti alloys) used for this test were received in the as-cast state. Characterisations of the alloys were done using Scanning Electron Microscope with Energy Dispersive X-Ray (SEM-EDX) to determine the chemical compositions of the alloys. Electrochemical measurements were carried out by conducting Potentiodynamic Polarization Tests at Open Circuit Potential and tribocorrosion tests were carried out using a ball-on-disc tribometer to simulate the wear conditions while a potentiostat was used to record the changes in current during the process. A three-electrode configuration test set-up was used for both the electrochemical and tribocorrosion tests and Phosphate Buffered Saline (PBS) was used to simulate the body fluid encountered by these alloys in the

human body. Characterization of the wear behaviour of these alloys was conducted after the tests using a Scanning Electron Microscope (SEM) to obtain images of the wear morphology, SEM-EDX to obtain the chemical composition on both the worn and unworn surfaces and a roughness meter to measure the surface roughness of both worn and unworn surfaces to determine the volume of wear loss.

**Structure of the Thesis** – The first part of this thesis is the introduction of the study, and it consists of the background of the study, aims and objectives, brief description of the research scope and a brief description of the experimental methodology. Chapter one contains the literature review which gives the theoretical concepts supporting the research topic, which will include a review of hip replacement surgeries, titanium alloys for load bearing implant applications, biocompatibility of titanium alloys, corrosion properties of titanium alloys, tribological properties of titanium alloys and tribocorrosion properties of titanium alloys. Chapter two gives the materials, material preparation methods, characterization and testing procedures used in getting the required information. The findings or outcomes (results) obtained from the procedures adopted in chapter two are described and presented in chapter three. These results are discussed in chapter four, which consists of the electrochemical and tribocorrosion properties of the alloys and characterization of the alloys before and after wear. This aims to extensively analyse all the results obtained and rationalise them against information obtained from the review of literature. Chapter five contains the conclusions, where all the details obtained from the research are summarised and recommendations for further work on these alloys are presented.

## CHAPTER 1 - LITERATURE REVIEW

### 1.1 Introduction

The literature review chapter contains an assessment of the literature related to the current study. To start with, biomaterials mainly metallic biomaterials with a focus on those used for load bearing orthopaedic applications are reviewed. Furthermore, titanium and its alloys are reviewed with emphasis on mechanical properties and biocompatibility of titanium and its alloying elements. In addition, corrosion resistance, wear and tribocorrosion behaviour in general and those specific to titanium and its alloys are reviewed.

### 1.2 Biomaterials

A prevalent attribute of biomaterials is that they are biocompatible i.e., they are compatible with the living tissues they are interacting with. There have been different definitions for biomaterials according to different subject experts. The Clemson University Advisory Board for Biomaterials defines biomaterials as “a systemically and pharmacologically inert substance designed for implantation within or incorporation with living systems” [8]. According to the National Institutes of Health (NIH) Consensus Conference, a *biomaterial* is defined as any substance (other than a drug) or combination of substances, synthetic or natural in origin, which can be used for any period of time, as a whole or as a part of a system which treats, augments, or replaces any tissue, organ, or function of the body. In other words, biomaterials are materials that can be implanted into the body to perform biological functions of living structures such as bone, cartilage, or tendons by repairing them or acting as a substitute [9]. Metals, polymers, ceramics, composites, and even living cells and tissues can be candidates for biomaterials. A few examples of biomaterials are contact lenses, pacemakers, heart valves, orthopaedic devices etc. For metals to be considered as biomaterials, there must possess certain properties to ensure that they can be implanted into the human body without any adverse effect and rejection for a long time. The fundamental properties of these implants are exceptional biocompatibility, good corrosion resistance, appropriate mechanical properties, excellent wear resistance, and osseointegration [8].

#### 1.2.1 Metallic Biomaterials used for Load-Bearing Implant Applications

The use of metals as orthopaedic implants is not a novel concept, and this is due to the ever-increasing demand for materials that can be used to replace damaged tissue and as such constant studies are being undertaken on how to improve them. Some of the most common causes of orthopaedic conditions are osteoarthritis, rheumatoid arthritis, osteonecrosis, fractures, tumours, and trauma. The most common implant component is the total hip replacement seen in Figure 1.

Image removed due to copyright restriction.

*Figure 1: Components of total hip replacement [10]*

Total hip replacements can deliver considerable reduction in arthritic pain as well as increased mobility to help the patient get back to walking without aids and withstand the weight of the patient. Therefore, materials used for total hip replacement must possess excellent load bearing properties. Metals have been increasingly used as hip replacements because of their excellent ability to withstand substantial loads. Total hip replacements consist mainly of three components: the stem, head, and acetabular component (Figure 1). The stems of most implants are made from metals such as stainless steel, CoCr or Ti alloys, the head is made from CoCr alloys or ceramic materials and the acetabular component can be made from metals or a mixture of polyethylene and a metal [11].

Titanium alloys are used to make the modular neck and femoral stem of implants because of their good mechanical properties, excellent corrosion resistance and biocompatibility.

### 1.3 Titanium and its Alloys

Compared with other metals such as stainless steel and cobalt based alloys used as implant biomaterials, titanium and its alloys possess excellent properties such as lower young's modulus, superior biocompatibility, and better corrosion resistance. From early 1970s, titanium and its alloys have been used for biomedical implants fabrication with commercially pure titanium (Cp-Ti) and Ti-6Al-4V being the most used [12].

Although Cp-Ti and Ti-6Al-4V have many properties that make them favourable for use as implant materials, there are still some issues associated with them. Some such issues worthy of mention are the presence of vanadium in Ti-6Al-4V which has been reported to be cytotoxic and high elastic modulus when compared to human bone [4, 13] which can lead to stress shielding, eventual loss of bone and implant loosening [14, 15]. To overcome these issues (mostly the toxicity), a new generation of titanium alloys were developed, one of which is Ti-



6Al-7Nb [16] in which the toxic vanadium has been replaced with niobium which has been found to be biocompatible [17].

Titanium and its alloys possess certain properties that ensure they can be implanted into the human body and perform well for a long time without much adverse effects and possible rejection. Some of these properties are excellent biocompatibility, exceptional mechanical properties, good corrosion resistance and excellent wear resistance.

### 1.3.1 Mechanical Properties of Titanium and its Alloys

Titanium alloys that will be implanted into the human body to augment or replace the functions of living tissues must be able to perform as well as the tissue it will be replacing (for instance bone). One of such area of performance is the mechanical property. Some of the mechanical properties of implants that determine their biomechanical compatibility are toughness, hardness, tensile strength, yield strength, young's modulus, and elongation [18]. These mechanical properties control the stress distribution at the interface between the bone and implant along with neighbouring bones [19]. Young's modulus is an important mechanical property because when using an implant because when an implant material has a higher Young's modulus than bone, the implant will bear more mechanical load than the bone causing biological responses around the implant site, such as atrophy, which reduces the lifespan of the implant and necessitates revision surgery [1, 14, 19, 20]. Such a situation is called the stress shielding effect. In an ideal situation, an implant with a similar Young's modulus to that of bone should be selected to replace the bone. From Table 1, the Young's modulus of bone is 10 – 30 GPa and from Table 2 the metallic material with the closest Young's modulus is titanium alloys at 105 -110 GPa, with other metallic materials having double this value. This suggests that the issue of stress shielding, and subsequent implant failure will be less when titanium implants are used then when other metallic implants are used.

Table 1: Mechanical properties of human bone [21]

	Yield strength, MPa	Ultimate strength, MPa	Elastic Modulus, GPa	Elastic strain, %	Density, g/cm <sup>3</sup>
Fibula	-	80-100	15.2-19.2	1.19-2.10	1.73-1.91
Humerus	-	149-151	15.6-16.1	1.90-2.20	1.72-1.77
Tibia	129	84-156.71	16.2-23.83	1.56-3.09	1.83-1.96
Femur	114.14	68-141	13.6-16.8	1.07-2.83	1.80-1.91

Table 2: Mechanical properties of some metallic biomaterials [9]

material	principal alloying elements (weight %)	elastic modulus (GPa)	yield strength (MPa)	ultimate strength (MPa)
stainless steel 316L	balance Fe 17–20 Cr 12–14 Ni 2–3 Mo max 0.03 C	205–210	170–750	465–950
CoCrMo F75	balance Co 27–30 Cr 5–7 Mo max 2.5 Ni	220–230	275–1585	600–1785
MP35N	balance Co 33–37 Ni 19–21 Cr 9–10.5 Mo			
Ti grade 4	balance Ti max 0.4 O	105	692	785
Ti4Al6V	balance Ti 5.5–6.5 Al 3.5–4.5 V	110	850–900	960–970
Ti6Al7Nb	balance Ti 6 Al 7 Nb	105	921	1024
Ti35Nb5Ta7Zr (TNZT)	balance Ti 35 Nb 5 Ta 7 Zr	55	530	590
NiTi	55.9–56.1 Ni balance Ti	20–70 (martensite) 70–110 (austenite)	50–300 (martensite) 100–800 (austenite)	755–960
TiNb	balance Ti 25–40 Nb	60–85	—	—

### 1.3.2 Biocompatibility of Titanium and its Alloys

Implants are designed in such a way that they will be in constant contact with living tissue and as such, it is imperative that the materials used to design them do not pose any danger to the surrounding living tissues. Biocompatibility covers a wide range of properties; from characteristics of bio-device to interactions of living tissues and cells with the implant material [22, 23]. Biocompatibility has been defined as “the ability to perform with an appropriate host response in a specific situation” [22, 23]. This definition is practical as the issue of biocompatibility goes beyond the safety of the material in the body but its usefulness because a biomaterial is expected to serve a particular purpose in the body while also being safe. Biocompatibility gives a measure of the success of an implant in the human body, and it is dependent on the reaction of the living systems to the presence of the foreign material. No material when implanted into living systems is fully unreactive or inert and to prevent any side effects, it is advisable that the use of these materials be limited to quantities that the living system can tolerate without an adverse effect. Titanium is a good choice for implant application because it is biocompatible and its presence in the human body is well tolerated [17]. Some of the alloying elements contained in titanium alloys have also been known to be biocompatible in the human body, with the exception of vanadium which has been reported to

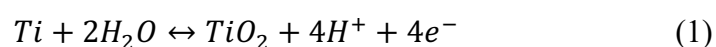
be cytotoxic [17]. Titanium has also been found to possess the ability to osseointegrate which is the “structural and functional connection between living bone and the surface of load bearing implant without intervening soft tissue” [24] and this can be said to be the primary goal of implant installation. Without this integration between bone and tissue, formation of fibrous tissue between the bone and the implant may occur and can lead to loosening of implants from bone [25, 26].

### 1.3.3 Corrosion of Titanium and its Alloys

Corrosion has been defined as an irreversible reaction between a material and its environment that leads to the degradation of the material [27]. Metallic biomaterials when implanted into the body inevitably react with their environment. The human body is made up of fluids which contain a solution of mostly sodium and chlorine, amino acids and other elements in trace quantities, thus making it an aggressive environment for implants [28]. Low corrosion resistance of implants in body fluid can result in liberation of antagonistic metal ions into the body by the implants and these ions can be very toxic and cause allergic reactions. These can be very harmful as they lead to implant loosening, and ultimately failure of the implant, thereby reducing the lifespan of the implant [25]. Reduction in lifespan of implants can result to having to perform a second surgery to remove the old implant and implant a new one. Also, corrosion of implants can lead to loss of human life as the products of corrosion can build up in tissues and can be transported to other parts of the human body and if not detected early can lead to poisoning.

Metals have been known to exhibit three responses in a corrosive environment and these responses are dependent on the metal and the environment. The first response is an immune response, where no corrosion of the metal occurs. The second is an active response, where corrosion of the metal occurs and metal loss or dissolution of the metal into the corrosive environment and the third response is the passive response, where the metal produces a protective oxide layer on its surface which reduces its corrosion rate [29, 30]. Titanium and its alloys have been known to display the third response in a corrosive environment because they can form a spontaneous protective oxide film on the titanium surface (a phenomenon known as passivation) according to the following reaction:

*Equation 1: Passivation equation for Ti*



Therefore, titanium and its alloys have excellent corrosion resistance. Another factor that contributes to the corrosion resistance properties of titanium alloys is the composition of the alloy. The presence of vanadium and niobium have been known to increase the corrosion

resistance of titanium alloys with niobium having a better effect on corrosion resistance than vanadium [31]. [31] reported that Ti-6Al-7Nb showed superior corrosion resistance than Ti-6Al-4V in lactic acid and NaCl solution and this was consistent with results obtained by [32] where tribocorrosion tests were conducted on titanium alloys produced by powder metallurgy in artificial saliva and results obtained by [3] where both alloys were tested in Phosphate Buffered Saline and Ti-6Al-7Nb was seen to display better corrosion resistance.

#### 1.3.4 Wear Behaviour of Titanium and its Alloys

Wear is the damaging, deformation, and gradual removal of materials from solid surfaces, and it occurs because of the relative motion between two rubbing surfaces. During wear, degradation of material takes place, and this can result in the failure of material. Wear has been reported to be one of the major reasons for implant failure and some of the applications of wear in the biomedical field are wear of dentures, heart valves, plates and screws in bone fracture repair etc. [26]. It is an important factor in the control and determination of the long-term clinical performance of metallic implants.

Metallic materials to be used for implant applications should have a high wear resistance and low coefficient of friction when sliding against body tissues. If these conditions are not met, the implant can loosen, and the wear debris generated can lead to inflammation and this is dangerous to the bone reinforcing the implant [26].

[33] investigated the wear behaviour of Cp-Ti, Ti-6Al-4V using a ball-on-flat fretting wear tester at a normal load of 10 N for 10,000 cycles at a frequency of 10 Hz and reported that the primary wear mechanism was tribomechanical abrasion, transfer layer formation and cracking. [34] also investigated the wear characteristics of high-strength titanium alloys and reported that the wear resistance of Ti-6Al-7Nb alloy was lower than that of the Ti-6Al-4V tested under various conditions of load and sliding speed.

Wear can be mechanical or chemical and the study of this phenomenon is known as tribology [26, 34, 35].

#### 1.3.5 Tribocorrosion of Titanium and its alloys

Tribocorrosion has been defined as the degradation of material surfaces when subjected to the combined action of mechanical loading which could be friction or abrasion, or erosion and corrosion attack caused by the environment which could be chemical or electrochemical reaction [36]. The mechanism of tribocorrosion is given by the schematic in Figure 2. Tribocorrosion is synergistic process between tribology and corrosion and this synergism results in material loss that is greater than the one expected if the degradation of the two processes acting individually were summed up [36]. During tribocorrosion, mechanical wear

might speed up the corrosion or electrochemical attack, or the electrochemical attack might speed up the mechanical attack. Therefore, to understand whether the corrosion attack speeds up the mechanical wear or the mechanical wear speeds up the corrosion attack, it is important to study the responses of the wear and corrosion and the influence of both during the tribocorrosion process [37].

Image removed due to copyright restriction.

*Figure 2: Basic concept of tribocorrosion [36]*

Metallic implants in the body are exposed to very intricate service conditions consisting of dynamic loading and relative motion with soft or hard tissues in contact. These conditions coupled with the corrosive nature of the body fluid can lead to tribocorrosion. It is therefore important that tribocorrosion studies of materials to be implanted into the human body be conducted.

Many studies have investigated the tribocorrosion behaviour of titanium and its alloys by influencing environmental variables such as pH, temperature, albumin content (in PBS), fluoride content (in saliva) etc [32, 35, 38, 39]. Caha et.al [4] studied the tribocorrosion behaviour of Ti-15Nb and Ti-40Nb alloys and compared with Ti-6Al-4V through an immersion period in saline solution for 21 days and reported that both alloys had poorer tribocorrosion resistance than Ti-6Al-4V alloy. Buciumeanu et.al [40] investigated the tribocorrosion behaviour of Ti-6Al-4V alloy produced using different manufacturing methods: casting, hot pressing (HP), or Laser Engineered Net Shaping (LENS) processes in PBS and reported that the LENS Ti-6Al-4V exhibited better tribocorrosion resistance while Toptan et.al [41] studied the tribocorrosion behaviour of selective laser melting produced Ti-6Al-4V in comparison with its hot pressed and commercial counterparts and reported that the processing routes did not show any significant difference on the tribocorrosion properties of the alloys.

#### 1.4 Research Gap

There has been a growing need for materials that can be used to replace and/or support biological structures, some of which are tissues, dental roots, organs etc. within the human body due to age,

illness or trauma. The materials to be used are required to have good mechanical properties; to withstand subjected stresses, excellent corrosion resistance; to withstand adverse reaction in the presence of corrosive agents, and excellent tribocorrosion resistance; to resist the combined forces of corrosive and mechanical wear. Titanium and its alloys have been used extensively for this application because they possess the afore-mentioned properties. The major titanium alloys extensively used are Ti-6Al-4V and Ti-6Al-7Nb and although much research has been conducted on the tribocorrosion properties of Ti-6Al-4V, very little research has been done on Ti-6Al-7Nb alloy. This is concerning because these alloys have been used in conditions where they are exposed to the combined and simultaneous effects of wear and corrosion without proper knowledge of how they will perform in these conditions. This is what this research paper aims to correct, to study the tribocorrosion behaviour of these two alloys in conditions that simulate those encountered by these alloys when implanted into the human body.

## CHAPTER 2 - METHODOLOGY

### 2.1 Introduction

In this chapter, the main features of the experimental work are described. The material preparation, alloy characterisation, electrochemical and tribocorrosion tests are presented. Finally, the surface damage characterisation techniques used (Scanning Electron Microscopy imaging and surface roughness measurement) are described.

### 2.2 Sample Preparation

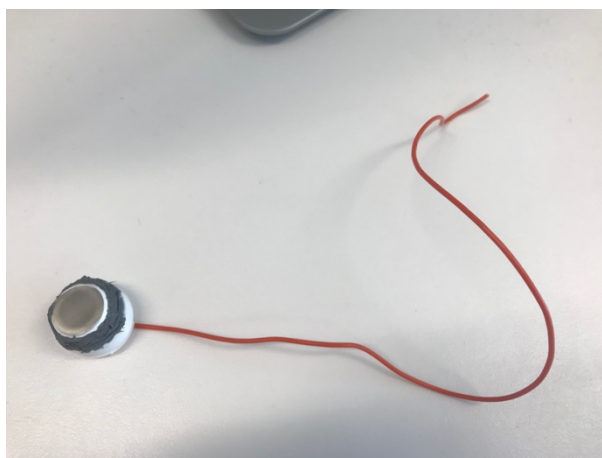
The materials used for this project were Ti-6Al-4V and Ti-6Al-7Nb alloys and were obtained in the as-cast form. The chemical compositions of these alloys were obtained using a Scanning Electron Microscope with Energy Dispersive X-ray and is presented in. The alloys were cut into discs of dimensions 16mm in diameter and 12mm in thickness using a Buehler Isomet 1000 precision saw seen in. The cut samples were then polished using Silicon Carbide papers of different grit sizes (240, 400 and 600) starting from coarse to fine to obtain a surface roughness of  $0.4 \mu\text{m}$  which is similar to those used in industrial applications. During polishing, care was taken to avoid any influence in the oxidation kinetics mechanism because of the level of plastic deformation. After polishing, the samples were rinsed using deionized water and then dried using compressed air.



Figure 3: Buehler Isomet saw

Prior to the electrochemical and tribocorrosion tests, the samples were cleaned using acetone to degrease and remove unwanted particles and masked using an electrochemical stop-off lacquer (Caswell sealer) to insulate the sample and expose only the required surface to the electrochemical and sliding conditions. A wire was attached to the bottom surface of the sample to aid electrical connection between the sample and the electrochemical testing equipment. A sample holder was designed using Autodesk Inventor and then 3D printed. The prepared sample was then placed in the sample holder and treated round with a T-Rex power

polymer gel to ensure good adhesion between the sample and holder and to prevent the electrolyte from leaking out as seen in Figure 4.



*Figure 4: Prepared sample*

A chamber or cell for carrying out the electrochemical tests was designed using Autodesk Inventor and then fabricated using a 3D printer (Figure 5). The printed chamber was treated using Techgrip adhesive to close out any holes to prevent leakage of electrolyte during testing.



*Figure 5: Electrochemical chamber for polarization tests*

The electrolyte used for the electrochemical and tribocorrosion tests to simulate the fluids encountered in the body was Phosphate Buffered Saline (PBS) [39, 42]. The PBS solution was made by dissolving tablets of Phosphate Buffered Saline in deionized water. A tablet of PBS was dissolved in 200 ml of deionized water.

The above method of sample preparation was carried out for both samples and for both electrochemical and tribocorrosion tests.

### 2.3 Electrochemical Corrosion Tests

Polarization tests were carried out to determine the kinetics of the alloys in PBS solution. For these experiments, an electrochemical cell with a three-electrode configuration was used. The three electrodes used were: the working electrode: the electrode in the electrochemical system on which the electrochemical reaction is occurring and in the case of this project were Ti-6Al-



4V and Ti-6Al-7Nb, the counter electrode: a platinum wire which was used to close the current circuit in the electrochemical cell, and the reference electrode: a silver/silver chloride (Ag/AgCl) electrode whose potential was known and was used as a point of reference in the electrochemical cell to control and measure the potential. During the tests, it was ensured that the counter electrode was larger than the working electrode in surface area so that it would not be a limiting factor in the kinetics of the electrochemical process because the current would be flowing between the working and counter electrodes. A Metrohm Autolab PGSTAT204 potentiostat running on NOVA 2.0 software was used to record the electrochemical measurements. The working electrode of each sample in the sample holder was placed in the electrochemical cell exposing an area of 2.01 cm<sup>2</sup> to the solution.

#### 2.3.1 Open Circuit Potential (OCP) Measurements

The open circuit potential is the spontaneous potential established between the working and reference electrodes at which anodic and cathodic reactions take place in the electrochemical system [43]. At OCP, the anodic and cathodic reaction rates are equal, making the net current zero. Tests conducted at OCP give qualitative indications of the metal state in an environment; be it active or passive. OCP was used to stabilize and create a steady state condition within the system and was conducted for 1800s with 0.1s interval time.

#### 2.3.2 Potentiodynamic Polarization Tests

The potentiodynamic polarization technique consists of setting a potential difference between the reference and working electrodes, at a potential difference range between the anodic and cathodic domains at a constant sweep rate and registering the produced current [43]. The current produced during this test represents the rate of reactions occurring on the working electrode; be it anodic or cathodic. This technique was selected because it gives valuable information on the corrosion processes taking place on the surface of the metal and is mostly used to evaluate the active/passive behaviour of materials at different potentials, thereby, providing information on the corrosion rate [43]. After stabilization at OCP, the linear polarization curves were recorded at a scan rate of 0.0002V/s, step of 0.0002V, interval time of 0.76294s for 12500s from a start potential (cathodic potential) of -1V to a stop potential (anodic potential) of 1V with respect to OCP. Polarization plots of current against potential were obtained during the tests. Each measurement was carried out on both alloys three times to ensure the reproducibility and repeatability of the experiments and then compared to each other.

## 2.4 Tribocorrosion Tests

Tribocorrosion tests were carried out by coupling the electrochemical system (potentiostat) to a tribometer. The tribometer was used to simulate the wear conditions experienced by implants in the body while the potentiostat was used to measure the current during the process. The tribometer used had a bidirectional motion and a ball-on-disc configuration (conforming to ASTM G133 standard) with the titanium alloy to be tested as the disc and zirconia ceramic as the ball. Tribocorrosion tests were carried out in conformity with the tribocorrosion synergistic approach stipulated in the ASTM G119.09 standard. A three-electrode configuration cell was also used for the tribocorrosion tests with the titanium alloys as the working electrode, Ag/AgCl as the reference electrode and platinum wire as the counter electrode. Care was taken to ensure that the reference electrode was placed no more than 1cm from the wear track to ensure accuracy in measurements [44] as seen in Figure 6.



*Figure 6: Tribocorrosion test setup*

Tribocorrosion tests were carried out at four different normal force levels of 3.5 N, 5.5 N, 10.6 N and 17.5 N which correspond to 580.2 MPa, 674.5 MPa, 839.4 MPa and 992.1 MPa contact pressures respectively after statistical analysis of the load cell using hertzian pressures was performed and three different sliding distances of 1mm, 3mm and 5mm for each contact pressure and 1Hz frequency of reciprocating motion for all contact pressures and sliding distances. These parameters were chosen as this work aims to explore a wide range of conditions experienced in the head and neck of implants in the hip joint and it has been reported

in literature that these conditions are common [45, 46]. All tests were carried out for 1800 cycles. During the experiments, the current was monitored using the NOVA 2.0 software on the potentiostat and a Lin-Mot Talk 6.9 software was used to control the tribometer. All tests on both alloys were repeated three times to check for reproducibility.

#### 2.4.1 Tribocorrosion Tests under Potentiostatic Conditions

This technique consists of imposing a fixed potential between the reference and working electrodes and measuring the current as a function of time to evaluate the rate of corrosion occurring at the material surface. This method was used for the tribocorrosion tests because imposing a fixed potential on sliding surfaces provides data on the effect of potential on the wear behaviour [43]. In this study, a constant anodic potential corresponding to the passive region [38] was applied to simulate the corrosion conditions experienced by alloys implanted in the body. At this potential, an oxide film whose thickness is controlled by the applied potential covers the alloy surface and serves to minimize the dissolution rate of the alloy and influence the wear response of the alloy [43].

The sequence for the potentiostatic tribocorrosion tests consisted of:

- Cathodic cleaning by applying a potential of -1.5V for 5 minutes to remove the oxide layer and this was to ensure that a new oxide layer was built at the level of potential the tests will be conducted at to ensure uniform conditions (REF).
- Stabilizing the samples at OCP for 5 minutes.
- Applying an anodic potential of 0.8V for 8 minutes until the oxide layer was formed at this potential.
- Adjusting the ball to touch the disc for 2 minutes to ensure stabilization.
- Sliding for 1800 cycles at a potential of 0.8V.

#### 2.5 Surface Characterization

Various tests were carried out after the tribocorrosion tests to characterise the wear behaviour, to study the effect of the tests on the surface of the alloy samples.

##### 2.5.1 SEM with EDX Analyser

The alloy surfaces before and after tribocorrosion tests were characterized using a FEI Inspect F50 Scanning Electron Microscope with Energy Dispersive X-Ray (Figure 7). The SEM chamber was vented to achieve the right pressure before placing the samples in the sample holder. The samples were mounted on a stub with carbon adhesive before placing in the sample holder. Adjustments were made to ensure the position of the sample was below 10cm and would not get hit by the door when closing the chamber. The chamber was then pumped to

achieve the optimum pressure within the chamber. Adjustments were made to the working distance, brightness, contrast, and magnification to ensure good image capture.

The quantitative analyses of the elemental constitution of the worn and unworn surfaces of the alloys were obtained from the same equipment using the EDAX software. Some of the parameters and the values used for capturing images are presented in Table 3 for reference purposes.

*Table 3: Operating parameters for SEM-EDX*

Parameter	Settings
Accelerating Voltage	20 kV
Spot Size	4
Beam Current	120 pA
Magnification	5000
Working Distance	9~10mm



*Figure 7: SEM instrument*

### 2.5.3 Surface Roughness Measurement

The surface roughness of the wear scar was determined using the Mitutoyo Roughness (Figure 8) meter which was used to compute the wear volume loss of the alloys after tribocorrosion.

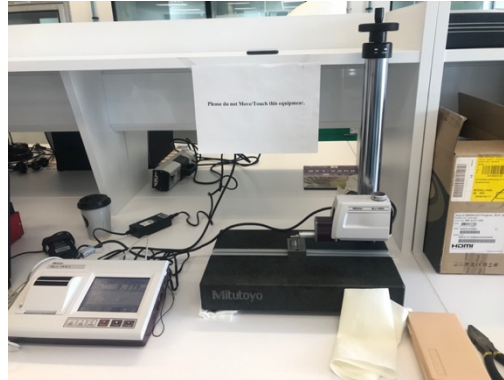


Figure 8: Roughness meter

## CHAPTER 3 - RESULTS

### 3.1 Introduction

In this chapter, the results of the investigation of corrosion behaviour, tribocorrosion behaviour and surface characterization before and after wear are presented. The results are presented as a comparison between both alloys: Ti-6Al-4V and Ti-6Al-7Nb. The results are presented in graphs, tables and images and a description of the trends is given.

### 3.2 Electrochemical Corrosion Results

A typical polarization curve usually consists of an active state, a passive state, and a trans-passive state. In the active state, the current density is known to increase swiftly as potential increases; this leads to the development of an oxide layer (passive film) on the surface of the metal. In the passive state, the current density reduces and remains at a certain level because of the protective effect of the oxide layer formed in the active state. On increasing the potential, the passive film will start to deteriorate and the current density will again increase swiftly [31].

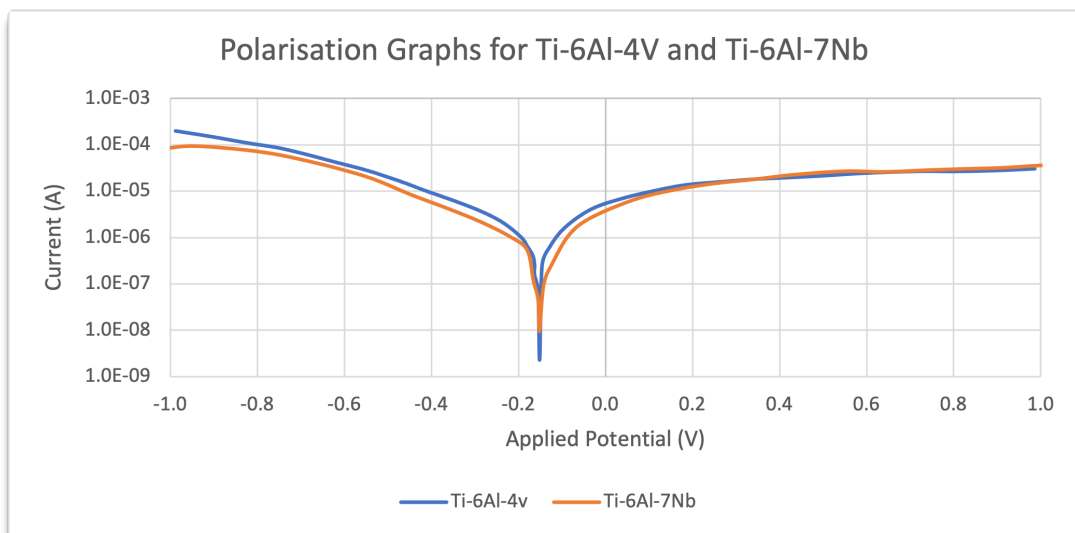


Figure 9: Polarization curve for Ti-6Al-4v and Ti-6Al-7Nb in PBS

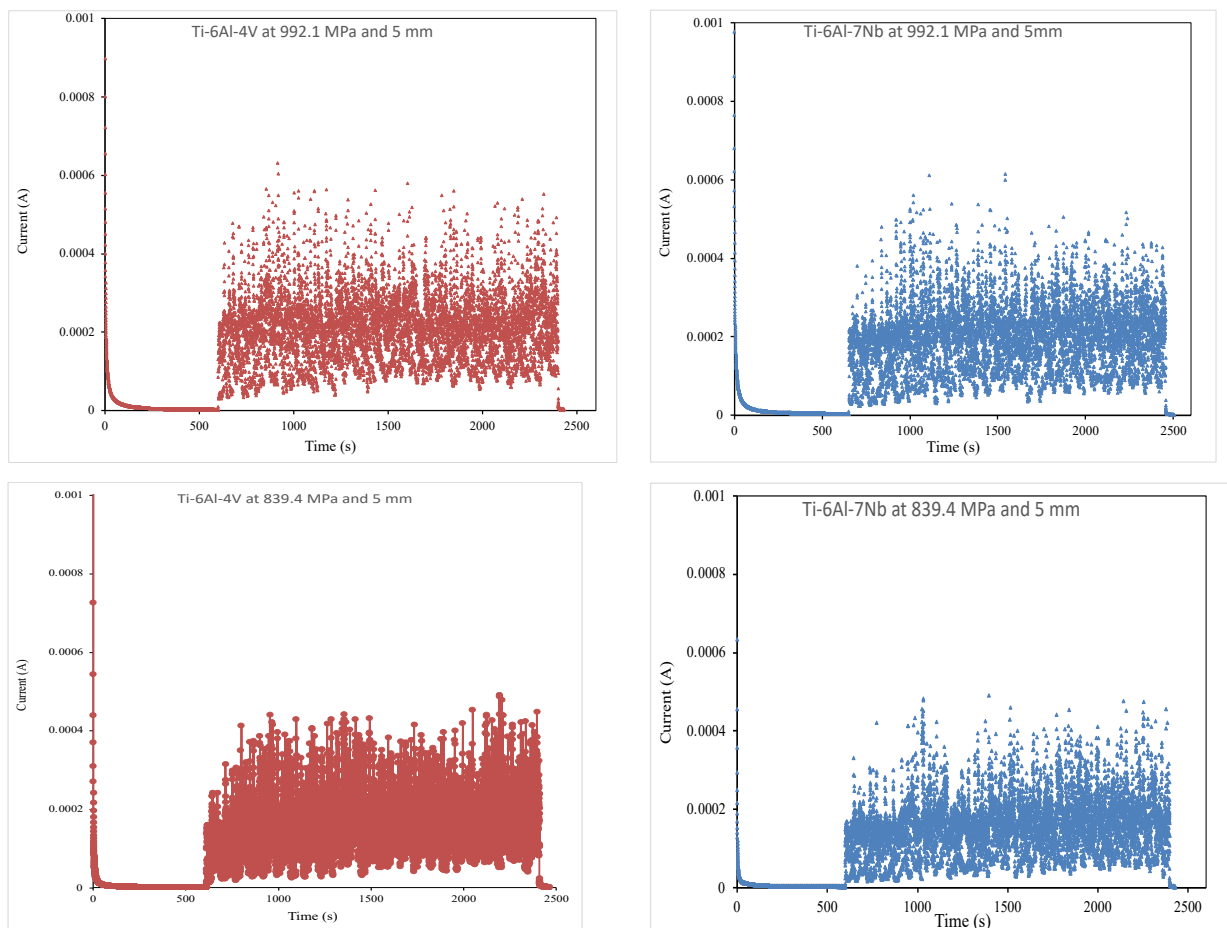
The polarization curves for both alloys in Figure 9 can be seen to follow the typical pattern for a polarization curve with three potential domains observed. The first domain is the cathodic domain, which includes all the potentials below the corrosion potential  $E_{CORR}$  (- 0.183 V) where the current density rises sharply and is given by the reduction of water and dissolved oxygen. The second domain corresponds to the potential range around  $E_{CORR}$  (- 0.183 V) where the transformation from cathodic to anodic current at the corrosion potential occurs. The third domain corresponds to the trans-passive domain where dissolution begins through the passive oxide film. From Figure 9, Ti-6Al-4V alloy exhibits higher current amplitudes when compared to Ti-6Al-7Nb.

## 3.2 Tribocorrosion Results

### 3.2.1 Tribocorrosion Graphs

Figure 10, Figure 11 and Figure 12 show the time evolution of current at an applied anodic potential of -0.8V before sliding, during sliding and after sliding of the titanium alloys against the zirconia ball in PBS solution. Before sliding, the whole surface of the alloy is passive and an anodic current of below 1  $\mu\text{A}$  is observed for both alloys at all conditions. At the initiation of sliding, a sharp increase in current was observed and a steady state value was reached after a few seconds. This increase in current is attributed to the mechanical removal of the passive film. The metal surface that is exposed experiences corrosion until the passive film is generated again. This continuous depassivation/repassivation will result in wear accelerated corrosion and consequently higher anodic current under constant potential conditions.

The current was observed to increase with increasing contact pressure and sliding distance for all studied alloys.



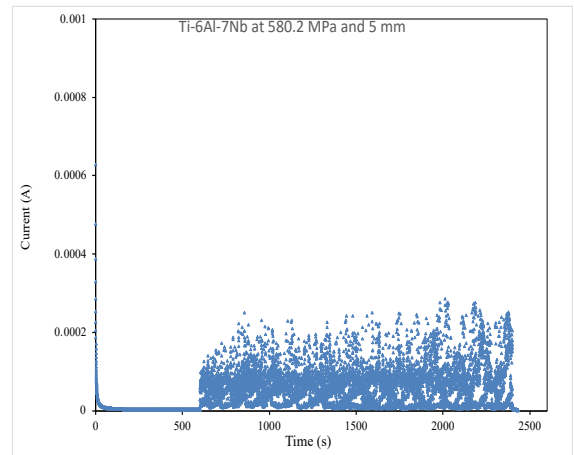
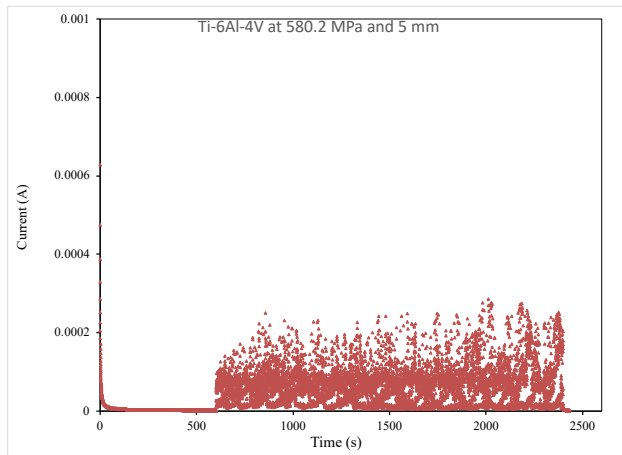
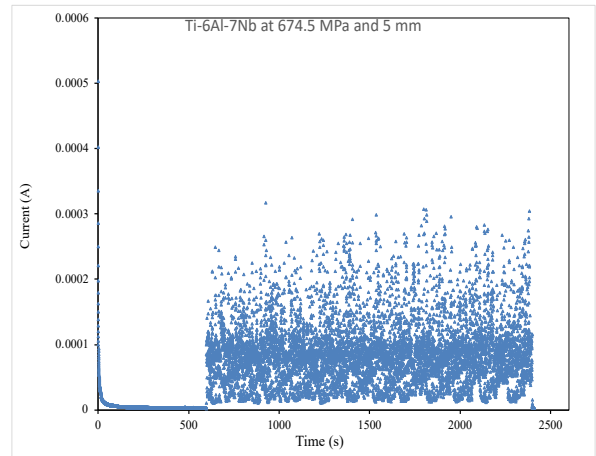
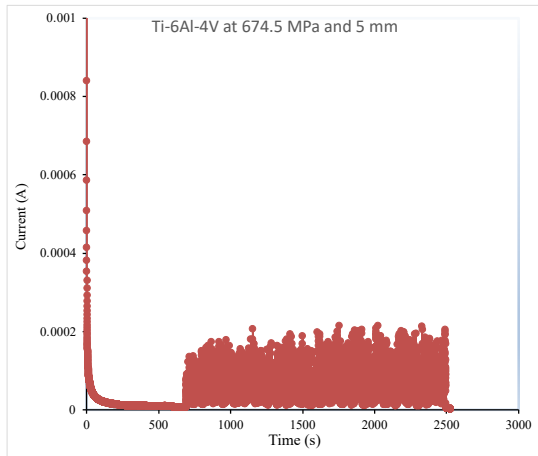
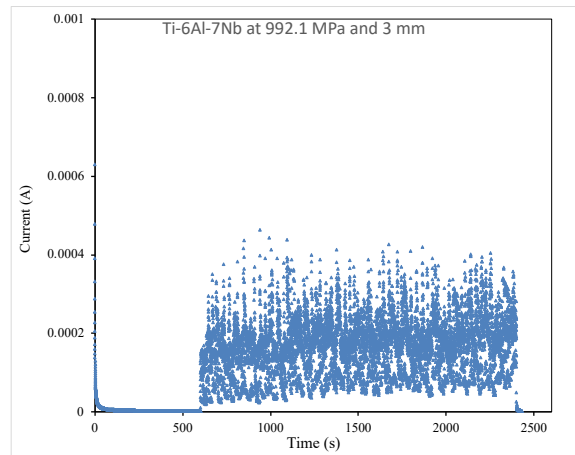
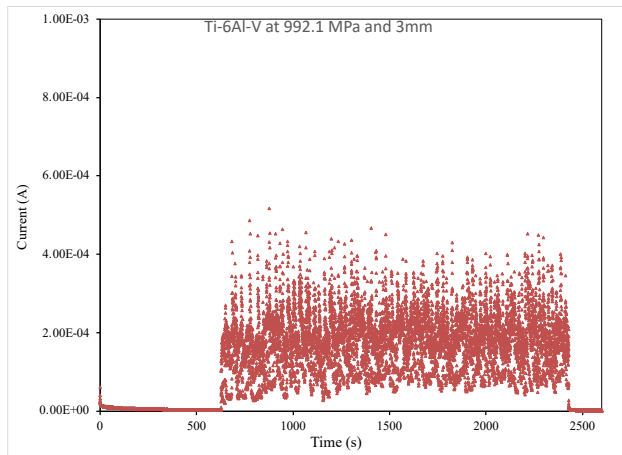


Figure 10: Current evolution with time of studied alloys at 5 mm sliding distance and all contact pressures





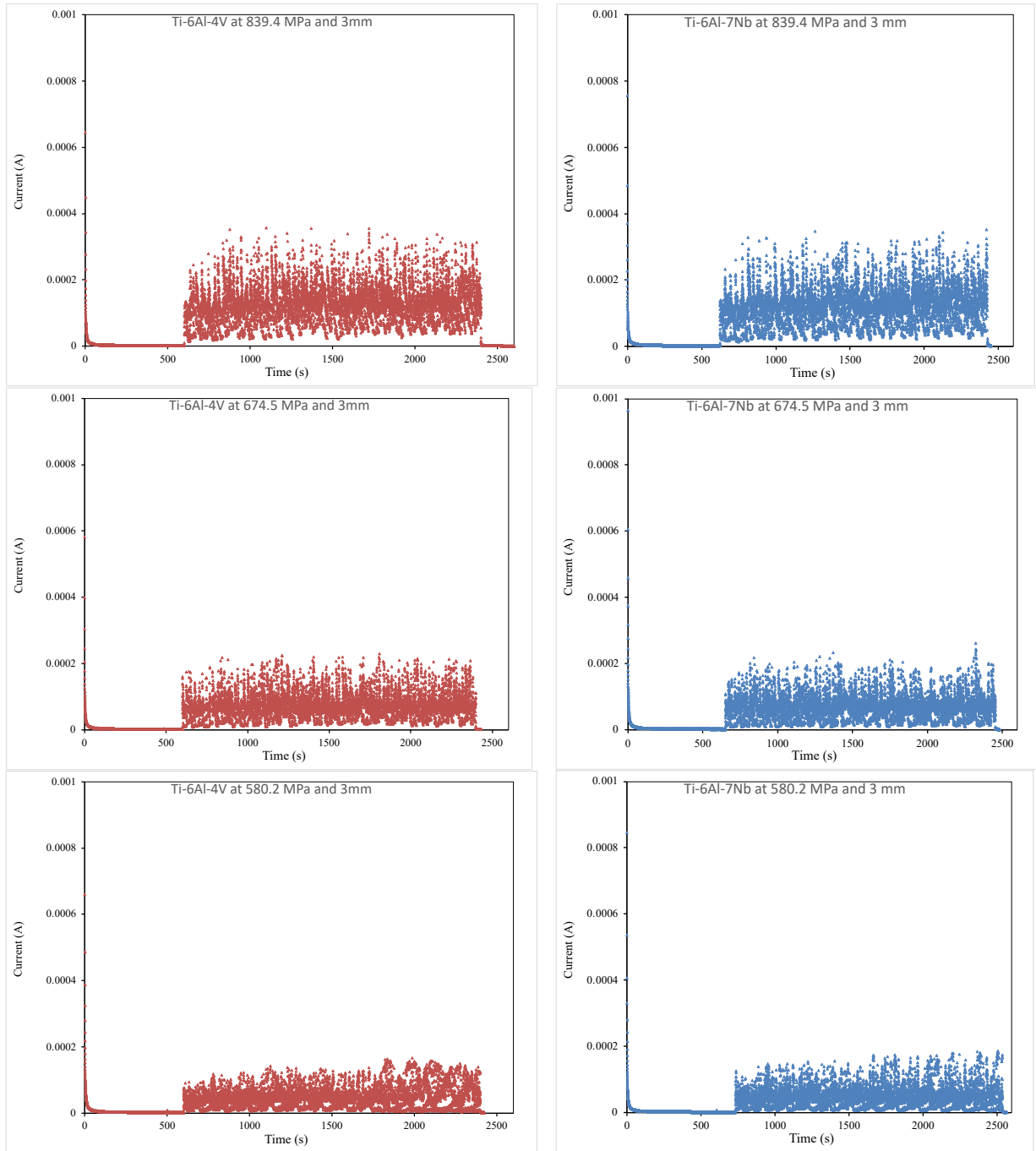


Figure 11: Current evolution with time of all alloys at 3 mm sliding distance and all contact pressures

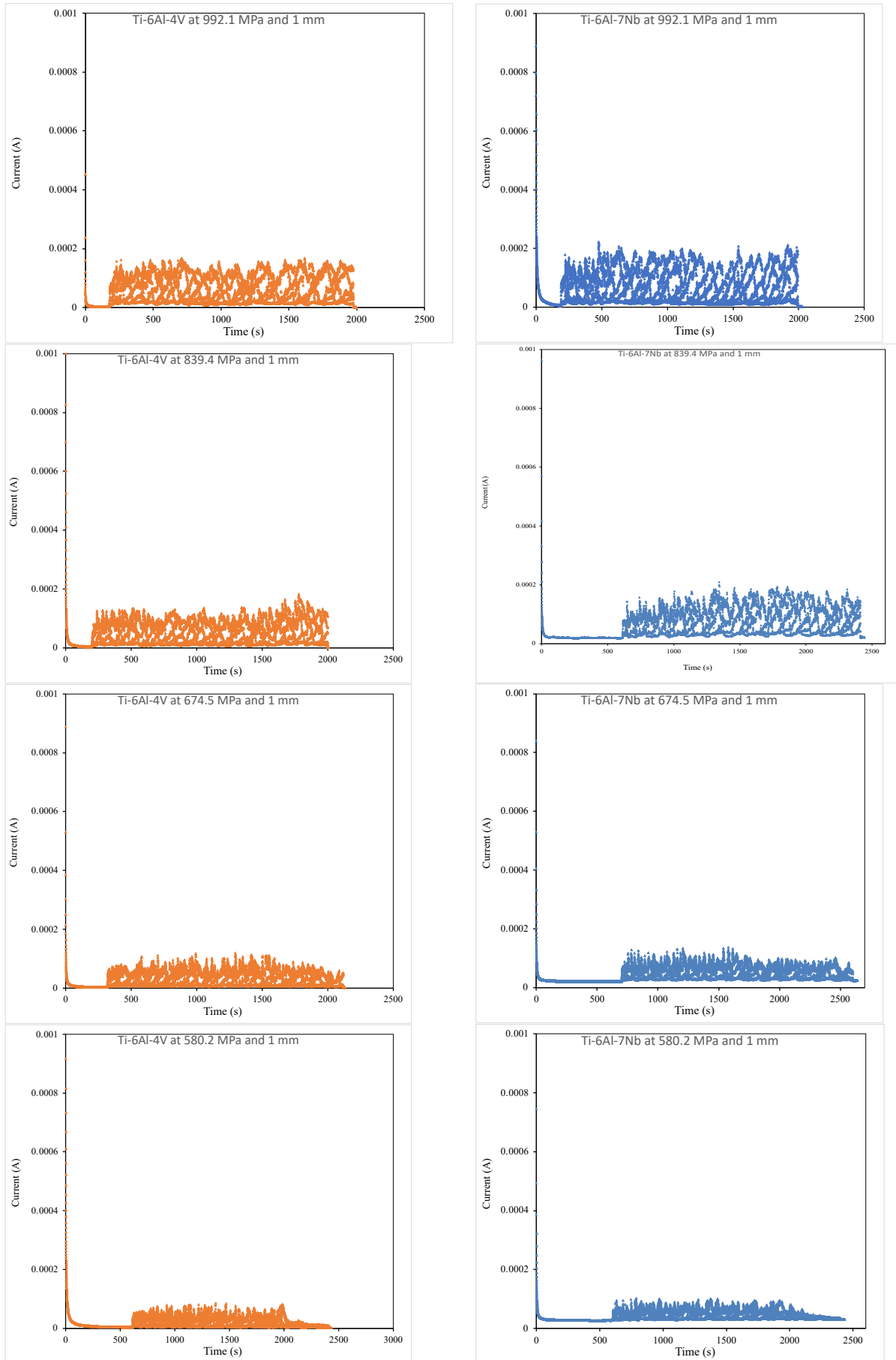


Figure 12: Current evolution with time of studied alloys at 1mm sliding distance and all contact pressures

### 3.2.2 Mean Current due to Tribocorrosion

The current due to sliding i.e., the current flowing in the wear track was computed by subtracting the current measured during sliding from the current measured before sliding and is presented in as the mean current due to sliding in Table 4: Mean Current due to sliding. The current before sliding was assumed to correspond approximately with the current flowing through the unworn surface since the worn area has a much smaller area than the total electrode area. Graphical representations of the mean current for both alloys at all conditions are also presented in Figure 13. From the graphs, it can be observed that as contact pressures and sliding distance increase, the mean current due to sliding also increases. It can also be seen that Ti-6Al-7Nb alloy had higher values of mean current at all contact pressures and sliding distance when compared to Ti-6Al-4V.

Table 4: Mean Current due to sliding

SLIDING DISTANCE (mm)	CONTACT PRESSURE (MPa)	MEAN CURRENT (A)	
		Ti-6Al-4V	Ti-6Al-7Nb
5mm	992.1	2.17E-04	2.03E-04
	839.4	1.65E-04	1.60E-04
	674.5	7.62E-05	8.62E-05
	580.2	5.29E-05	6.81E-05
3mm	992.1	1.83E-04	1.72E-04
	839.4	1.32E-04	1.27E-04
	674.5	5.54E-05	7.21E-05
	580.2	4.68E-05	4.97E-05
1mm	992.1	6.42E-05	9.30E-05
	839.4	5.20E-05	7.86E-05
	674.5	3.18E-05	5.50E-05
	580.2	2.27E-05	4.78E-05

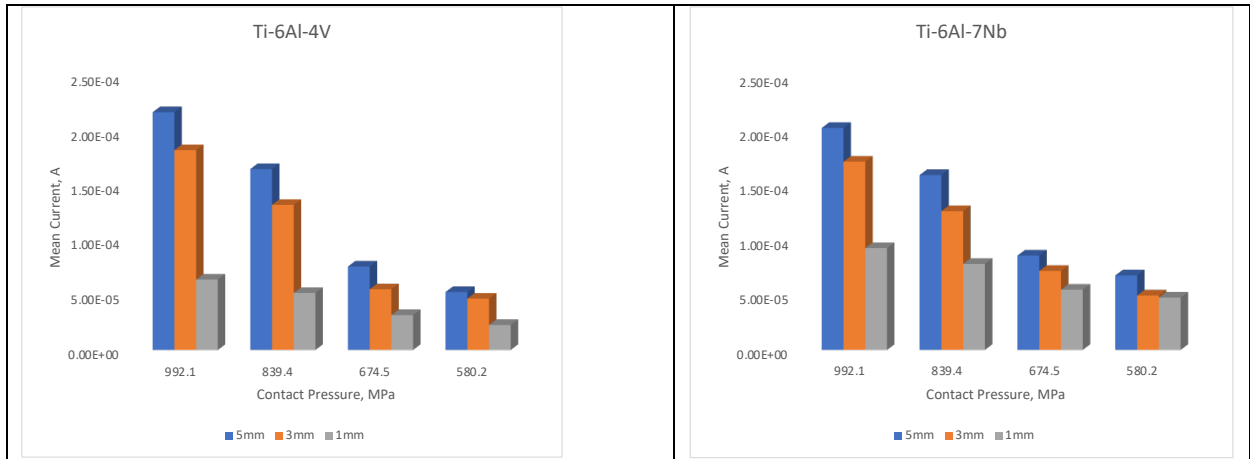


Figure 13: Graphical representation of mean current due to sliding

The chemical wear loss that occurred as a result of the anodic oxidation in the wear was calculated from the measured current using Faraday’s law:

Equation 2: Chemical wear loss equation

$$V_{chem} = \frac{I_{sliding} \times t \times M}{n \times F \times \rho} \quad (2)$$

Where M = atomic mass of alloy, 446.067g/mol for Ti-6Al-4V and 568.9792g/mol for Ti-6Al-7Nb

n = charge number for oxidation reaction (assumed to be 4)

F = Faraday constant (96,500 C/mol)

$\rho$  = density of alloy (4.4 g/cm<sup>3</sup>)

t = duration of rubbing, 1800 s.

The calculated chemical wear loss is presented in and it can be observed that increased with increasing contact pressures and sliding distance and Ti-6Al-7Nb exhibited higher chemical wear than Ti-6Al-4V under the same conditions.

Table 5: Chemical Wear Loss Values

SLIDING DISTANCE (mm)	CONTACT PRESSURE (MPa)	CHEMICAL WEAR LOSS (mm <sup>3</sup> )	
		Ti-6Al-4V	Ti-6Al-7Nb
5mm	992.1	1.03E-04	1.22E-04
	839.4	7.80E-05	9.65E-05
	674.5	3.60E-05	5.20E-05
	580.2	2.50E-05	4.11E-05
3mm	992.1	8.65E-05	1.04E-04
	839.4	6.24E-05	7.66E-05

	674.5	2.62E-05	4.35E-05
	580.2	2.21E-05	3.00E-05
1mm	992.1	3.04E-05	5.61E-05
	839.4	2.46E-05	4.74E-05
	674.5	1.50E-05	3.32E-05
	580.2	1.07E-05	2.88E-05

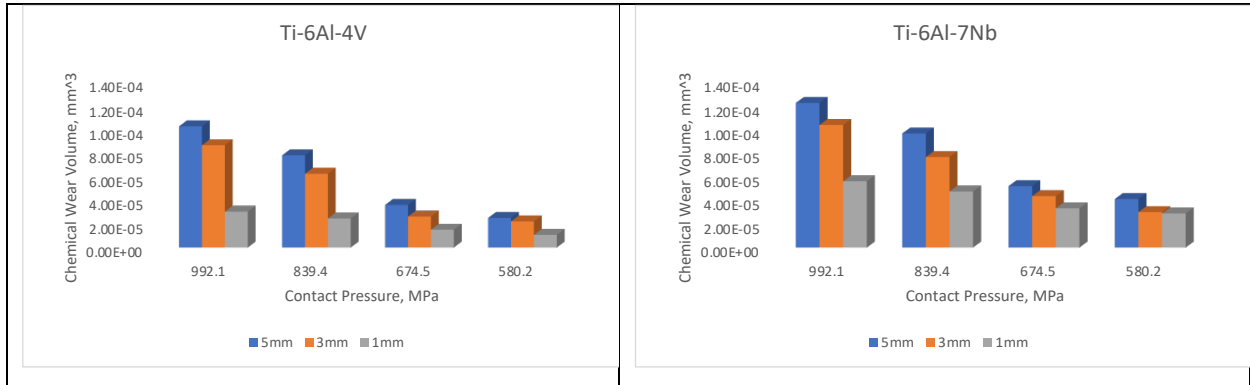


Figure 14: Chemical wear volume loss

### 3.3 Surface Roughness

The wear volume loss of the studied alloys was determined by computing the planimetric cross-sectional wear profile of the wear track based on the ASTM D7755-11 standard using the roughness meter. The wear volume of the studied alloys was computed using:

Equation 3: Wear volume equation

$$W_{v,flat} = \frac{\pi \cdot d_4^2 (d_3 - s)^2}{64} \cdot \frac{1}{R} + s \cdot W_{q,flat} \quad (3)$$

Where:

$d_3$  = the total length of wear track in sliding direction in mm,

$d_4$  = the width of the wear track in mm, and

$s$  = stroke in mm

and

Equation 4: Equation for  $R$

$$\bar{R} = \frac{d_4^3}{12 \cdot W_{q,flat}} \quad (4)$$

Where:

measured diameter  $d_4 = d_2$  in mm.

The calculated values for wear volume loss are presented in and it can be seen to follow the already established trend in this report of increasing with increasing contact pressures and sliding distance with Ti-6Al-7Nb exhibiting higher mechanical material loss than Ti-6Al-4V under the same conditions. Figure 15 gives a cross-section of one of the wear scars under conditions of contact pressure and sliding distance.

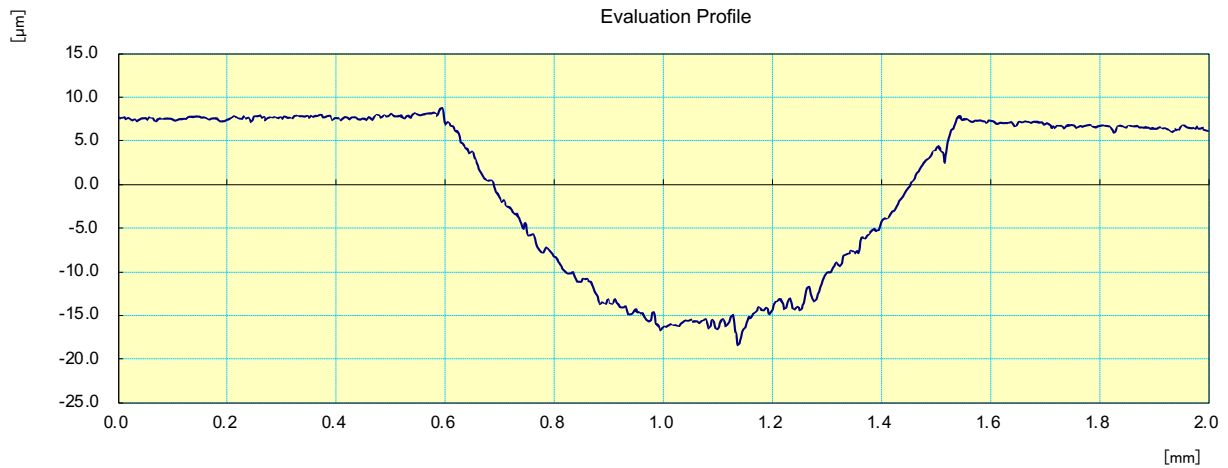


Figure 15: Cross-section of wear tracks

Table 6: Mechanical wear loss values

SLIDING DISTANCE (mm)	CONTACT PRESSURE (MPa)	MECHANICAL WEAR LOSS (mm <sup>3</sup> )	
		Ti-6Al-4V	Ti-6Al-7Nb
5mm	992.1	1.38E-05	1.43E-05
	839.4	8.31E-06	9.24E-06
	674.5	4.25E-06	4.81E-06
	580.2	3.36E-06	4.47E-06
3mm	992.1	1.07E-05	8.91E-06
	839.4	7.47E-06	6.82E-06
	674.5	2.62E-06	4.07E-06
	580.2	1.39E-06	2.85E-06
1mm	992.1	5.04E-06	5.82E-06
	839.4	3.44E-06	4.80E-06
	674.5	2.16E-06	3.65E-06
	580.2	1.10E-06	1.40E-06

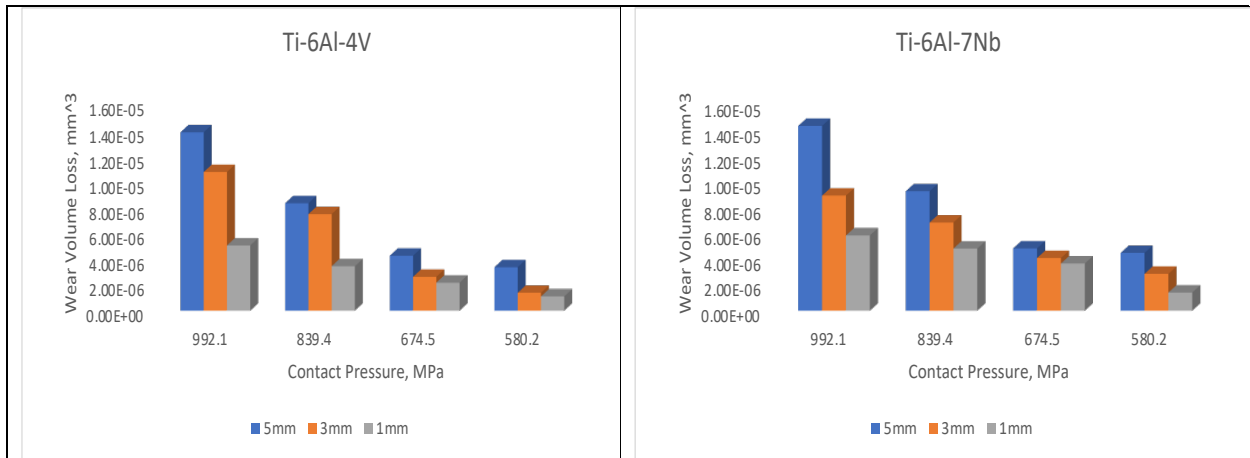


Figure 16: Mechanical Wear volume loss of studied alloys

The total volume corresponding to the loss of material during wear is expressed as:

Equation 5: Total volume equation

$$V_{total} = V_{chemical} + V_{mechanical} \quad (5)$$

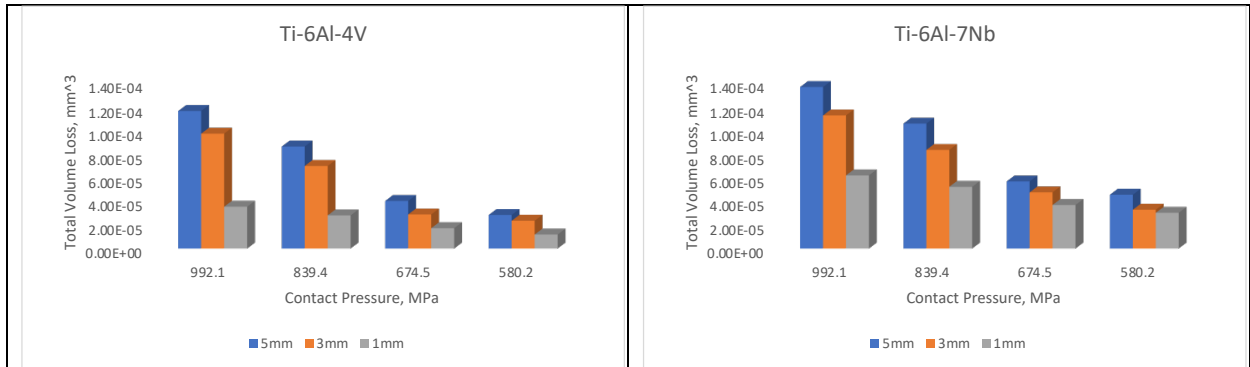
Where  $V_{chemical}$  is the chemical wear volume loss and  $V_{mechanical}$  is the mechanical volume loss. The computed values are shown in and the graphical representation is shown in. From both sets of representation, it can be seen that the total volume loss increases with increasing contact pressure and sliding distance and is higher for Ti-6Al-7Nb when compared to Ti-6Al-4V under the same conditions.

Table 7: Total Wear Loss Values

SLIDING DISTANCE (mm)	CONTACT PRESSURE (MPa)	TOTAL WEAR LOSS (mm <sup>3</sup> )	
		Ti-6Al-4V	Ti-6Al-7Nb
5mm	992.1	1.16E-04	1.37E-04
	839.4	8.63E-05	1.06E-04
	674.5	4.03E-05	5.68E-05
	580.2	2.84E-05	4.55E-05
3mm	992.1	9.72E-05	1.13E-04
	839.4	6.99E-05	8.34E-05
	674.5	2.88E-05	4.76E-05
	580.2	2.35E-05	3.28E-05
1mm	992.1	3.54E-05	6.19E-05

	839.4	2.80E-05	5.22E-05
	674.5	1.72E-05	3.68E-05
	580.2	1.18E-05	3.02E-05

Table 8: Total wear loss graph



### 3.4 SEM Imaging Results

From Figure 17, Figure 18, Figure 19, and Figure 20, the wear tracks show a predominantly abrasive mechanism which can be seen by the grooves on the entire scar length and is parallel to the direction of sliding. Isolated wear debris was observed on all worn surfaces. Not much difference was observed in the wear morphology of both alloys only that Ti-6Al-7Nb appeared to have deeper wear grooves.

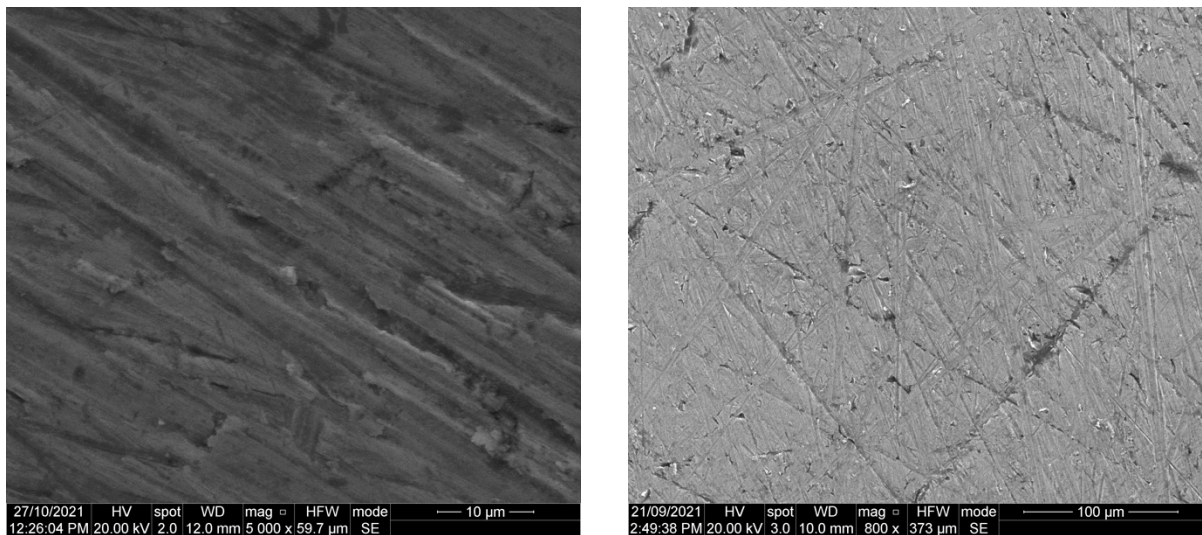


Figure 17: SEM images of unworn alloy surfaces with Ti-6Al-4V on the left and Ti-6Al-7Nb on the right



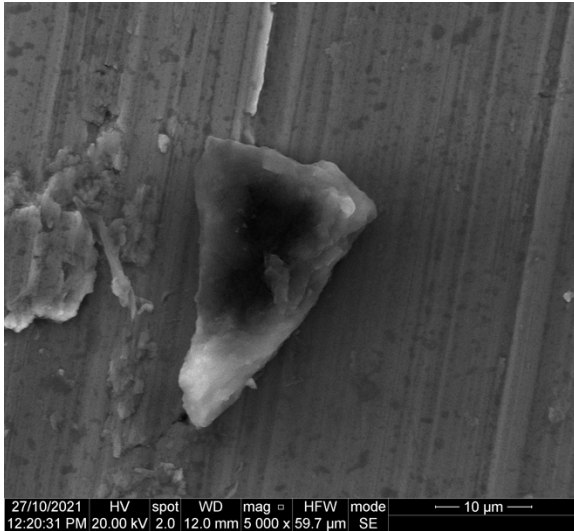


Figure 18: SEM images for worn surface at 992.1 MPa and 5 mm sliding distance with Ti-6Al-4V on the left and Ti-6Al-7Nb on the right

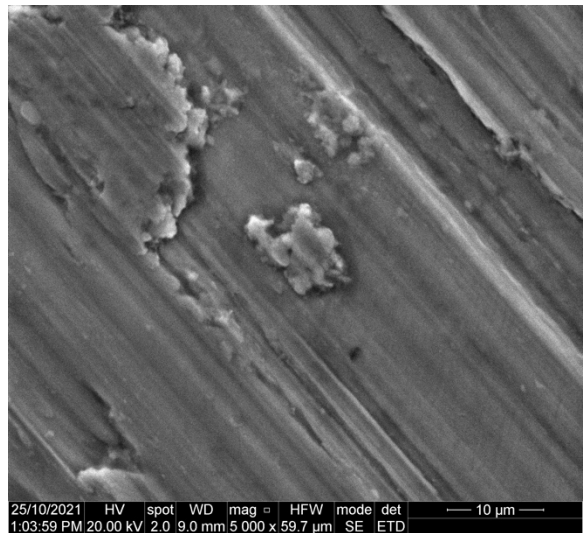
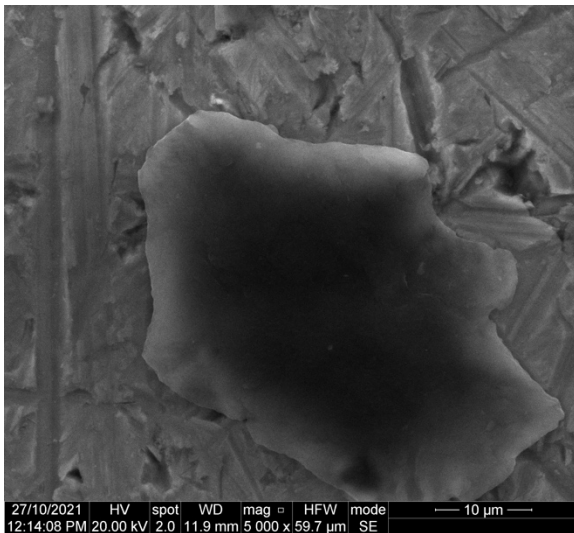


Figure 19: SEM images for worn surfaces at 580.2 MPa and 5 mm sliding distance with Ti-6Al-4V on the left and Ti-6Al-7Nb on the right

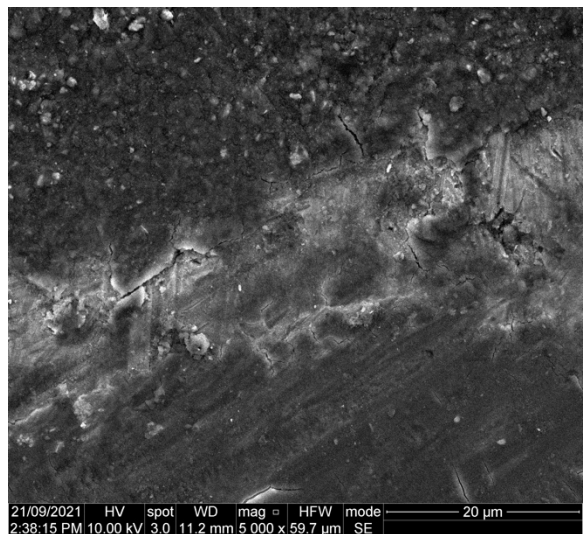
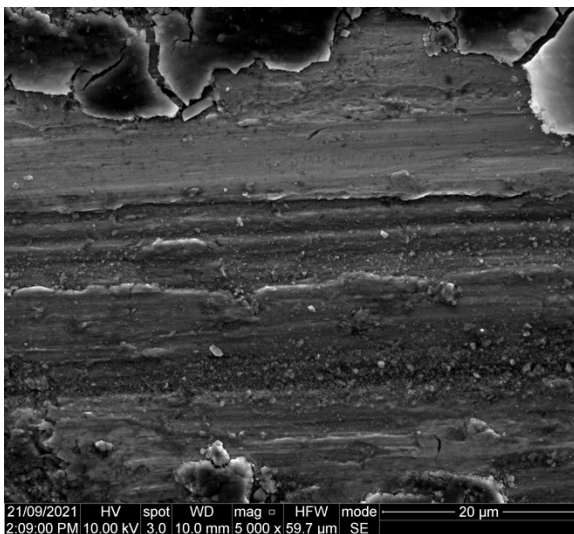


Figure 20: SEM images of worn surface at 992.1 MPa and 1 mm sliding distance with Ti-6Al-4V on the left and Ti-6Al-7Nb on the right

### 3.5 EDS Results

The chemical composition of elements in both alloys obtained through EDS are presented in Figure 21, Figure 22, Table 9, Table 10 and Table 11. The compositions presented in Table 9 were obtained from the unworn surface of the Ti-6Al-7Nb alloy and the overall compositional weightage for the three major elements in the alloy (Ti, Al and V) are very close to the expected composition of the element. This is also the case for the Ti-6Al-4V alloy as seen in Table 11. However, for the unworn and worn surfaces of both alloys, large amounts of oxygen can be found along with trace levels of other elements.

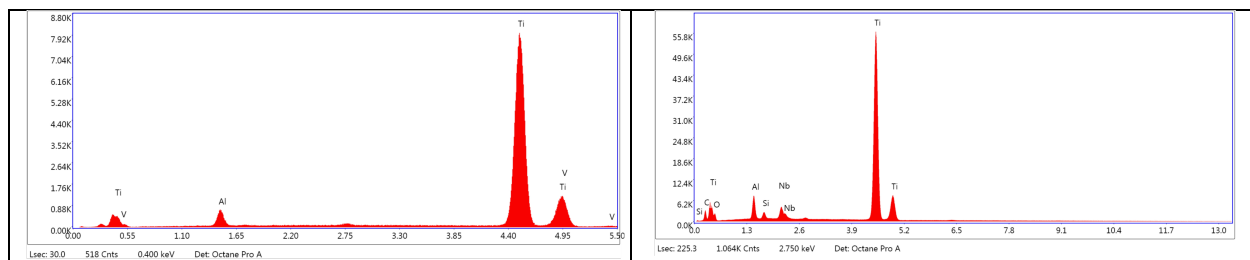


Figure 21: EDS analysis for unworn surface of studied alloys with Ti-6Al-4V on the left and Ti-6Al-7Nb on the right

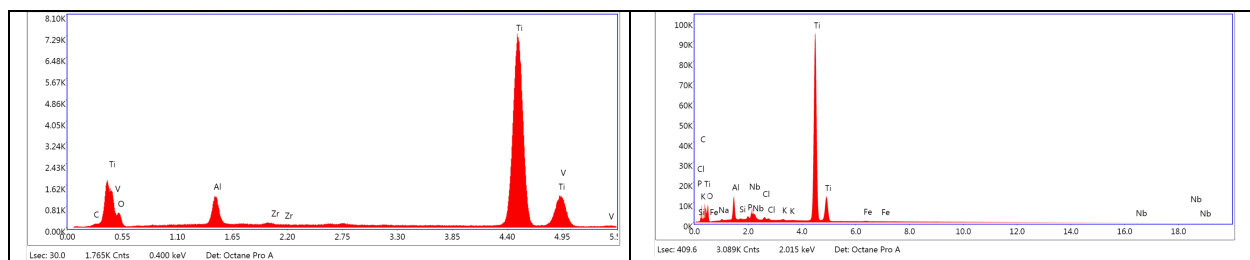


Figure 22: EDS analysis for worn surface of studied alloys with Ti-6Al-4V on the left and Ti-6Al-7Nb on the right

Table 9: Chemical composition of unworn Ti-6Al-7Nb

Spectrum	Ti wt%	Al wt%	Nb wt%	O wt%	C wt%	Na wt%	Si wt%	P wt%	Cl wt%	K wt%	Fe wt%
1	23.83	2.10	1.99	16.67	50.26	1.26	1.03	0.42	0.34	0.85	-
2	71.90	3.58	10.50	7.18	5.63	-	-	-	-	-	0.95
3	57.93	2.14	2.97	16.30	19.03	-	0.78	-	-	-	-
4	82.49	5.90	5.00	6.60	9.34	-	-	-	-	-	-
Average	59.0375	3.43	5.115	11.6875	21.065	1.26	0.905	0.42	0.34	0.85	0.95

Table 10: Chemical composition of worn Ti-6Al-7Nb

Spectrum	30iw t%	Al wt%	Nb wt%	O wt%	C wt%	Na wt%	Si wt%	P wt%	Cl wt%	K wt%	Fe wt%
1	64.32	3.60	3.57	17.08	9.67	0.54	0.02	0.43	0.37	0.18	0.23
2	72.66	3.52	3.40	14.40	4.59	0.57	0.01	0.30	0.21	0.17	0.15
3	37.60	2.39	2.68	13.61	40.65	0.75	0.16	0.75	0.56	0.55	0.29
4	56.87	4.37	4.52	21.21	9.34	0.93	0.17	0.80	0.87	0.43	0.49
Average	57.8625	3.47	3.5425	16.575	16.0625	0.6975	0.09	0.57	0.5025	0.3325	0.29

Table 11: Chemical composition of worn and unworn Ti-6Al-4V

Spectrum	3Iwt%	Al wt%	V wt%	O wt%	Zr wt%	Na wt%	S wt%	P wt%	Cl wt%	K wt%	Fe wt%
worn	72.95	5.38	2.29	17.17	0.33	-	-	-	-	-	-
unworn	92.56	3.85	3.59	-	-	-	-	-	-	-	-

## CHAPTER 4 - DISCUSSION

### 4.1 Introduction

This chapter discusses the experimental results on corrosion behaviour, tribocorrosion behaviour and surface characterization before and after wear. All results are extensively analysed and accounted for against information obtained from review of related literature. The behaviours of both alloys are analysed and discussed for comparison.

### 4.2 Corrosion Behaviour Analysis

Titanium alloys have been known for their ability to spontaneously passivate in most electrolytes by the formation of an oxide layer when reaction with water takes place. From the corrosion results obtained in Figure 9, the corrosion resistance of Ti-6Al-7Nb alloy was found to be better than Ti-6Al-4V alloy in PBS solution and this is consistent with results obtained by Kobayashi et.al who investigated the corrosion behaviour of both alloys in NaCl and lactic acid [31]. The anodic polarization test was conducted to assess the corrosion resistance of these alloys accurately. As seen in Figure 9, the passive state was very conspicuous affirming the repassivating property of this alloy. However, no peak was observed at the critical passivation holding current density which is a common occurrence in anodic polarization curves of titanium alloys when testing in neutral electrolytes, which was the case with PBS [31].

### 4.3 Tribocorrosion Behaviour Analysis

The current values during tribocorrosion are represented in Figure 10, Figure 11, Figure 12, and Figure 13. Before sliding, it was observed that the current values recorded were very low suggesting that no electrochemical corrosion was occurring at that point and this is because of the passive oxide layer formed on the surface of the titanium alloys [4, 6]. This behaviour was observed for both alloys under all conditions. It was observed that as soon as sliding started, there was a rapid increase in the anodic current values under all conditions which suggests that corrosion kinetics increase at those points due to the mechanical damage of the passive film [41]. As soon as the sliding stopped, the anodic current dropped rapidly to the stabilization values observed before sliding and this is because of the recovery of the passive film [6, 32]. This property of titanium and its alloys to repassivate takes place swiftly as evidenced by the stabilization of the current as soon as sliding stopped.

The current amplitude was observed to increase as sliding distance and contact pressure increased and this is because at higher sliding distances and contact pressures, the surface of the alloys undergoes rapid wear which breaks down the passive film as soon as it forms. The higher the contact pressure and sliding distance, the higher the wear and the faster the passive layer is broken down before it can completely form [4, 6, 38].

Mean sliding current, chemical volume loss, mechanical volume loss and total volume loss were higher in Ti-6Al-7Nb than Ti-6Al-4V indicating that the latter had better wear and tribocorrosion resistance properties.

#### 4.4 Surface Characterization

The observed worn surfaces after characterisation were typical for titanium and its alloys as reported by [32, 41]. Grooves that were parallel to the direction of sliding were observed in both alloys and oxidised patches were also seen on both alloys. These suggest that the wear experienced by both alloys were predominantly adhesive in nature and localised wear debris was observed for both alloys. The presence of the oxidised patches was also reinforced from the EDS results in Table 10 and Table 11 where large chemical compositions of oxygen were found on both worn and unworn surfaces of both alloys. The presence of oxygen reinforces the passivation properties of these alloys which is the formation of a protective oxide film in the presence of water. On close inspection, Ti-6Al-7Nb appeared to have deeper wear scars further giving evidence to the poorer wear and tribocorrosion resistance properties of this alloy Figure 18.

#### 4.5 Limitations

As stated previously, not much research has been conducted on the tribocorrosion behaviour of Ti-6Al-7Nb, therefore, it was difficult to compare the results obtained from the research with other work. As a result, the discussion section of this work mainly focused on comparing the results obtained with previous reported behaviour of Ti-6Al-4V. Based on these comparison, the major findings were that Ti-6Al-4V presented better tribocorrosion resistance than Ti-6Al-7Nb in terms of general, chemical and mechanical wears while Ti-6Al-7Nb presented better corrosion resistance than Ti-6Al-4V.

## CHAPTER 5 - CONCLUSION

### 5.1 Conclusions

In this study, the corrosion and tribocorrosion behaviour of Ti-6Al-4V and Ti-6Al-7Nb were conducted by electrochemical techniques in PBS, an electrolyte used to simulate body fluids and the following conclusions can be drawn from the results obtained:

- Ti-6Al-7Nb has better corrosion resistance properties than Ti-6Al-4V in simulated body fluids (PBS)
- Ti-6Al-4V has better tribocorrosion resistance than Ti-6Al-7Nb under the same conditions of contact pressures and sliding motions
- Ti-6Al-4V has better wear resistance properties than Ti-6Al-7Nb under the same conditions of contact pressure and sliding distance
- Increasing contact pressure reduces tribocorrosion resistance in both alloys
- Increasing sliding distance reduces tribocorrosion resistance in both alloys.

### 5.2 Recommendations for Future Work

From the results obtained, both alloys have their strengths: better corrosion resistance in Ti-6Al-7Nb and better tribocorrosion resistance in Ti-6Al-4V but a concerning aspect of these alloys is their toxicity as they both contain aluminium which has been linked to many neurological disorders such as Alzheimer's and cytotoxicity in the case of vanadium in Ti-6Al-4V. As such, further research has to be conducted to replace these toxic elements with non-toxic ones while still maintain their exceptional properties. Another aspect that could be improved upon is the large difference between the Young's modulus of these alloys and that of bones which can lead to stress-shielding effect. Studies need to be conducted on reducing the Young's modulus of these alloys to bring them closer to that of the human bone.



## REFERENCES

1. Lee, T., et al., *Breaking the limit of Young's modulus in low-cost Ti-Nb-Zr alloy for biomedical implant applications*. Journal of Alloys and Compounds, 2020. **828**: p. 154401.
2. Jiang, B., et al., *Effects of Nb and Zr on structural stabilities of Ti-Mo-Sn-based alloys with low modulus*. Materials Science and Engineering: A, 2017. **687**: p. 1-7.
3. Khan, M., R.L. Williams, and D.F. Williams, *The corrosion behaviour of Ti-6Al-4V, Ti-6Al-7Nb and Ti-13Nb-13Zr in protein solutions*. Biomaterials, 1999. **20**(7): p. 631-637.
4. Caha, I., et al., *Degradation behavior of Ti-Nb alloys: Corrosion behavior through 21 days of immersion and tribocorrosion behavior against alumina*. Corrosion Science, 2020. **167**: p. 108488.
5. Ehtemam-Haghighi, S., et al., *Microstructure, phase composition and mechanical properties of new, low cost Ti-Mn-Nb alloys for biomedical applications*. Journal of Alloys and Compounds, 2019. **787**: p. 570-577.
6. Correa, D., et al., *Tribocorrosion behavior of  $\beta$ -type Ti-15Zr-based alloys*. Materials Letters, 2016. **179**: p. 118-121.
7. Hee, A.C., et al., *Tribo-corrosion performance of filtered-arc-deposited tantalum coatings on Ti-13Nb-13Zr alloy for bio-implants applications*. Wear, 2018. **400**: p. 31-42.
8. Park, J. and R.S. Lakes, *Biomaterials: an introduction*. 2007: Springer Science & Business Media.
9. Navarro, M., et al., *Biomaterials in orthopaedics*. Journal of the royal society interface, 2008. **5**(27): p. 1137-1158.
10. Nguyen, D.-n., *Simulation and experimental study on polishing of spherical steel by non-Newtonian fluids*. The International Journal of Advanced Manufacturing Technology, 2020. **107**(1): p. 763-773.
11. Saini, M., et al., *Implant biomaterials: A comprehensive review*. World Journal of Clinical Cases: WJCC, 2015. **3**(1): p. 52.
12. Elias, C., et al., *Biomedical applications of titanium and its alloys*. Jom, 2008. **60**(3): p. 46-49.
13. Konushkin, S.V., et al., *Study of the physicochemical and biological properties of the new promising Ti-20Nb-13Ta-5Zr alloy for biomedical applications*. Materials Chemistry and Physics, 2020. **255**: p. 123557.
14. Biesiekierski, A., et al., *Investigations into Ti-(Nb, Ta)-Fe alloys for biomedical applications*. Acta biomaterialia, 2016. **32**: p. 336-347.
15. Li, P., et al., *Microstructural and mechanical properties of  $\beta$ -type Ti-Mo-Nb biomedical alloys with low elastic modulus*. Journal of Alloys and Compounds, 2020. **815**: p. 152412.
16. Bombač, D., et al., *Review of materials in medical applications Pregled materialov v medicinskih aplikacijah*. RMZ-Materials and Geoenvironment, 2007. **54**(4): p. 471-499.
17. Biesiekierski, A., et al., *A new look at biomedical Ti-based shape memory alloys*. Acta biomaterialia, 2012. **8**(5): p. 1661-1669.
18. Santos, P.F., et al., *Microstructures, mechanical properties and cytotoxicity of low cost beta Ti-Mn alloys for biomedical applications*. Acta biomaterialia, 2015. **26**: p. 366-376.
19. Akahori, T., et al., *Improvement in fatigue characteristics of newly developed beta type titanium alloy for biomedical applications by thermo-mechanical treatments*. Materials Science and Engineering: C, 2005. **25**(3): p. 248-254.
20. Fellah, M., et al., *Structural, tribological and antibacterial properties of ( $\alpha$ +  $\beta$ ) based ti-alloys for biomedical applications*. Journal of Materials Research and Technology, 2020. **9**(6): p. 14061-14074.

21. Li, Y., et al., *New developments of Ti-based alloys for biomedical applications*. Materials, 2014. **7**(3): p. 1709-1800.
22. Williams, D., *General concepts of biocompatibility*, in *Handbook of biomaterial properties*. 2016, Springer. p. 563-570.
23. Williams, D.F., *Progress in Biomedical Engineering: Definitions in Biomaterials*. 1987: Elsevier.
24. Brånemark, P., H. Gröndahl, and B. Brånemark, *Why osseointegration would work and how it did in the first patients treated. Basic facts and philosophical thoughts*. The osseointegration book: From calvarium to calcaneus. Berlin (Germany): Quintessence, 2005.
25. Geetha, M., et al., *Ti based biomaterials, the ultimate choice for orthopaedic implants—a review*. Progress in materials science, 2009. **54**(3): p. 397-425.
26. Hussein, M.A., A.S. Mohammed, and N. Al-Aqeeli, *Wear characteristics of metallic biomaterials: a review*. Materials, 2015. **8**(5): p. 2749-2768.
27. Popoola, A., O. Olorunniwo, and O. Ige, *Corrosion resistance through the application of anti-corrosion coatings*. Developments in corrosion protection, 2014. **13**(4): p. 241-270.
28. Manam, N., et al., *Study of corrosion in biocompatible metals for implants: A review*. Journal of Alloys and Compounds, 2017. **701**: p. 698-715.
29. Davis, J.R., *Surface engineering for corrosion and wear resistance*. 2001: ASM international.
30. Hailing, J., *Encyclopedia of tribology: By C. Kijdas, SSK Harvey and E. Wilusz, published by Elsevier, Amsterdam, 1990, 500 pp., price US \$156.50 (Dfl. 305.00)*. 1991, Elsevier.
31. Kobayashi, E., et al., *Mechanical properties and corrosion resistance of Ti-6Al-7Nb alloy dental castings*. Journal of Materials Science: Materials in Medicine, 1998. **9**(10): p. 567-574.
32. Licausi, M.-p., *Analysis of tribocorrosion behavior of biomedical powder metallurgy titanium alloys*. 2017, Universitat Politècnica de València.
33. Choubey, A., B. Basu, and R. Balasubramaniam, *Tribological behaviour of Ti-based alloys in simulated body fluid solution at fretting contacts*. Materials Science and Engineering: A, 2004. **379**(1-2): p. 234-239.
34. Fella, M., et al., *Friction and wear behavior of Ti-6Al-7Nb biomaterial alloy*. 2013.
35. Ferreira, D.F., et al., *Synergism between mechanical wear and corrosion on tribocorrosion of a titanium alloy in a Ringer solution*. Journal of Materials Research and Technology, 2019. **8**(2): p. 1593-1600.
36. Mathew, M., et al., *Significance of tribocorrosion in biomedical applications: overview and current status*. Advances in tribology, 2009. **2009**.
37. Revathi, A., et al., *Degradation mechanisms and future challenges of titanium and its alloys for dental implant applications in oral environment*. Materials Science and Engineering: C, 2017. **76**: p. 1354-1368.
38. Çaha, I., et al., *Corrosion and tribocorrosion behavior of Ti-40Nb and Ti-25Nb-5Fe alloys processed by powder metallurgy*. Metallurgical and Materials Transactions A, 2020. **51**(6): p. 3256-3267.
39. Dimah, M.K., et al., *Study of the biotribocorrosion behaviour of titanium biomedical alloys in simulated body fluids by electrochemical techniques*. Wear, 2012. **294**: p. 409-418.
40. Buciumeanu, M., et al., *Tribocorrosion behavior of additive manufactured Ti-6Al-4V biomedical alloy*. Tribology International, 2018. **119**: p. 381-388.



41. Toptan, F., et al., *Corrosion and tribocorrosion behaviour of Ti6Al4V produced by selective laser melting and hot pressing in comparison with the commercial alloy*. Journal of Materials Processing Technology, 2019. **266**: p. 239-245.
42. Pina, V.G., et al., *Tribocorrosion behavior of beta titanium biomedical alloys in phosphate buffer saline solution*. Journal of the mechanical behavior of biomedical materials, 2015. **46**: p. 59-68.
43. López-Ortega, A., J. Arana, and R. Bayón, *Tribocorrosion of passive materials: a review on test procedures and standards*. International Journal of Corrosion, 2018. **2018**.
44. Instruments, G., *Two-, three-, and four-electrode experiments*. Application Note, 2011.
45. Neto, M.Q. and W.M. Rainforth, *Effect of potential and microstructure on the tribocorrosion behaviour of beta and near beta Ti alloys I*. Biotribology, 2020. **24**: p. 100141.
46. Wang, L., et al., *Contact mechanics studies of an ellipsoidal contact bearing surface of metal-on-metal hip prostheses under micro-lateralization*. Medical engineering & physics, 2014. **36**(4): p. 419-424.